Archival Report

Biological Psychiatry: CNNI

Longitudinal Changes in Infant Attention-Related Brain Networks and Fearful Temperament

Courtney A. Filippi, Alice Massera, Jiayin Xing, Hyung G. Park, Emilio Valadez, Jed T. Elison, Dana Kanel, Daniel S. Pine, Nathan A. Fox, and Anderson Winkler

ABSTRACT

BACKGROUND: Anxiety disorders may partly stem from altered neurodevelopment of attention-related networks. Neonatal alterations in resting-state functional connectivity (rsFC) among the dorsal attention network (DAN), frontoparietal network (FPN), salience network (SN), and default mode network (DMN) relate to fearful temperament, a risk marker for anxiety. Nevertheless, few studies have examined the development of these networks beyond the first months of life, particularly in fearful infants. In this study, we examined how changes in these networks during the first 2 years of life relate to fearful temperament.

METHODS: Using data from the Baby Connectome Project (from 180 infants across 396 sessions), we conducted independent component analysis to extract rsFC among the DMN, SN, DAN, and FPN. Longitudinal modeling characterized 1) age-related changes (slope) in rsFC through age 2 years, 2) the relationship between rsFC change (slope) and fearfulness at age 2 years, and 3) the relationship between rsFC and fearfulness trajectories (slope and intercept) during the first 2 years of life.

RESULTS: Age-related decreases occurred in DAN-FPN and DMN-SN rsFCs. Smaller decreases in DAN-FPN rsFC over time related to greater fear at age 2 and to increases in fearfulness over time. High initial DAN-FPN rsFC and low initial DAN-SN rsFC also related to increasing fearfulness over time.

CONCLUSIONS: This study provides the first evidence that changes in attention-related brain networks are related to early-life fearfulness, a robust early-life risk marker of anxiety.

https://doi.org/10.1016/j.bpsc.2025.07.003

Anxiety disorders are prevalent (1), arise early (2), and involve altered attention (3–5), possibly through dysfunction in several large-scale brain networks (e.g., the dorsal attention network [DAN], frontoparietal network [FPN], salience network [SN], and default mode network [DMN]) (6). Because fearful infants are at risk for anxiety and exhibit altered resting-state functional connectivity (rsFC) among these networks (7–12), anxiety may reflect aberrant development of attention-related brain networks (13). However, few studies have considered how these brain networks change after the first months of life, particularly among infants at risk for anxiety (14). In the current study, we link changes in attention-related brain networks over the first 2 years of life to fearful temperament, an anxiety risk marker.

Fearful temperament, like anxiety, involves perturbations in attention (15–18). Whether it is measured observationally or with parent report, fearfulness robustly predicts later anxiety (19–24), particularly when fearfulness is persistent (25,26). Although fearfulness fluctuates over the first year of life, by toddlerhood, individual differences in fearful temperaments stabilize (27–29). Thus, it is crucial to examine links between the development of fearfulness and attention-related networks.

The SN, FPN, DMN, and DAN support attention across the lifespan (3,30–35), including during infancy. While the SN directs attention to salient environmental stimuli (36), the FPN and DAN align attention to a person's goals (37,38). Together, the DAN, FPN, and SN sustain and reorient attention during demanding cognitive tasks (37,39). Unlike the SN, FPN, and DAN, the DMN is most active when not engaged in a particular cognitive task (40). For this reason, the DMN is thought to underlie internally oriented attention (41,42). In patients with anxiety, individual differences in engagement of these networks during attention-demanding tasks is paralleled by alterations in these networks at rest (43). While few task-based functional magnetic resonance imaging (fMRI) studies have examined infants (44), newborns at high risk for anxiety show greater engagement in the SN, FPN, and DMN than newborns at low risk when attending to salient stimuli (45,46). Newborn studies have also shown that greater rsFC within the SN (7,9,47), less rsFC within the DMN (10,12), and less rsFC between the DAN-DMN, -SN, and -FPN (8) are associated with infant fearfulness. Greater within-network rsFC during infancy reflects increased synchronization and specialization among brain regions (6), whereas reductions in between-network rsFC may reflect increasing network segregation and functional differentiation (6).

The consistency across studies of infants and patients with anxiety could indicate that anxiety risk is characterized by early alterations in rsFC and limited change in rsFC over time.

ISSN: 2451-9022

However, this hypothesis remains untested. To date, no study has evaluated how changes in rsFC relate to changes in fearfulness using longitudinal MRI and behavioral assessments (6,11,48–50). However, one report has mapped how rsFC changes over the first 2 years of life relate to emotional outcomes (11). This study found that greater amygdala-DMN and amygdala–visual network rsFC and less amygdala–sensorimotor network rsFC (from ages 1–2) were associated with greater anxiety at age 4 (11). While promising, <30 infants in this study provided complete data, and therefore there is a need for larger studies.

In the current study, we characterized the development of attention-related brain networks using the BCP (Baby Connectome Project) data (49). We obtained high-quality rsFC from 180 infants across 396 sessions, with most infants providing data for 2 or 3 time points. rsFC among 4 attention-related networks (i.e., DMN, SAN, DAN, and FPN) was quantified, and between-network connectivity was extracted. This study had 3 aims: first, to characterize age-related changes in rsFC across all network pairs; second, to evaluate the relationship between rsFC change (slope) and fearfulness at age 2; and third, to evaluate co-trajectories of fearfulness and rsFC across the first 2 years of life. In this study, we took a hypothesis-driven approach to characterizing the neurodevelopmental origins of fearful temperament.

METHODS AND MATERIALS

Participants

A total of 209 full-term infants were scanned between birth and 60 months (University of Minnesota site of the BCP) (49). Infants were excluded if they were preterm (gestational age <37 weeks), had low birth weight (<2000 g), had contraindication to MRI, the mother experienced severe pregnancy and/or delivery complications or reported illicit drug use during pregnancy, or the infant had a first-degree relative with a known neurodevelopmental disorder or a medical condition affecting development. Infants were also excluded if their parents could not provide informed consent in English or if the child was adopted. All parents/guardians provided informed consent prior to data collection. This study was approved by the institutional review board.

Several infants were excluded for insufficient high-quality MRI data (see Quality Control and Data Loss for details). In total, 180 infants had sufficient high-quality MRI data for inclusion in group-level analyses (see Table 1 for demographics). Of these, 114 infants (63%) contributed high-quality longitudinal data: 59 infants with 2 time points, 19 infants with 3 time points, 26 infants with 4 time points, 9 infants with 5 time points, and 1 infant with 6 time points. In total, we utilized MRI data from 396 MRI sessions ($\text{mean}_{\text{MRI sessions per infant}}$ = 2.2, SD = 1.25, range = 1–6) (see Figure 1 for postnatal age distribution details). Infants included in the final analysis did not differ from infants excluded on race/ethnicity ($p > .51$), maternal education ($p = .1$), income ($p > .066$), or sex ($p > .34$) (see the Supplement for more details).

MRI Data

Acquisition. MRI data were acquired on a 3T Siemens Prisma scanner. At each MRI session, T1-weighted (TR = 2400 ms, TE = 2.24 ms, flip angle = 8°, 0.8 mm isotropic), T2-weighted (TR = 3200 ms, TE = 564 ms, flip angle = variable°, 0.8 mm isotropic), and resting-state (TR = 800 ms, TE = 37 ms, flip angle = 52°, 2 mm isotropic) scans were obtained. At processing onset, we identified 518 complete MRI sessions. An additional 101 MRI sessions were attempted but resulted in insufficient data for processing (7 infants had insufficient T1-weighted scans, 3 infants were missing T2-weighted scans, and 91 were missing resting-state data).

Table 1. Demographics for Sample of Infants With High-Quality Imaging Data from the Baby Connectome Project (*N* = 180)

	n or *n* (%)
Sex	
Female	91
Male	89
Ethnicity/Race	
Latino/Hispanic and Asian	0 (0%)
Latino/Hispanic and Black	1 (0.55%)
Latino/Hispanic and more than 1 race	3 (1.7%)
Latino/Hispanic and White	8 (4.4%)
Non-Hispanic and Asian	2 (1.1%)
Non-Hispanic and Black	0 (0%)
Non-Hispanic and more than 1 race	28 (15.6%)
Non-Hispanic and White	137 (76.1%)
Not answered/White	1 (0.55%)
Maternal Education	
Some high school	1 (0.55%)
High school	1 (0.55%)
Some college	13 (7.2%)
College	69 (38.3%)
Some graduate school	11 (6.1%)
Graduate school	80 (44.4%)
Not reported	5 (2.8%)
Income	
<$25,000	2 (1.1%)
$25,000–$34,999	3 (1.7%)
$35,000–$49,999	6 (3.3%)
$50,000–$74,999	34 (18.9%)
$75,000–$99,999	34 (18.9%)
$100,000–$149,999	54 (30%)
$150,000–$200,000	28 (15.6%)
>$200,000	18 (10%)
Not reported	1 (0.5%)

Preprocessing fMRI. Data from the 518 MRI sessions were submitted to Nibabies (version 21.0.2), an infant equivalent of fMRIPrep, for preprocessing. Anatomical preprocessing used intensity normalization, skull stripping, tissue segmentation (i.e., gray matter, cerebrospinal fluid [CSF], and white matter [WM]), and spatial normalization to University of North Carolina age-specific template and Montreal Neurological Institute (MNI) space (51,52). Functional data preprocessing included slice timing correction, estimation of head-motion parameters, spatiotemporal filtering, field map rigid registration to the target echo-planar imaging reference run, correction for susceptibility distortions and head motion,

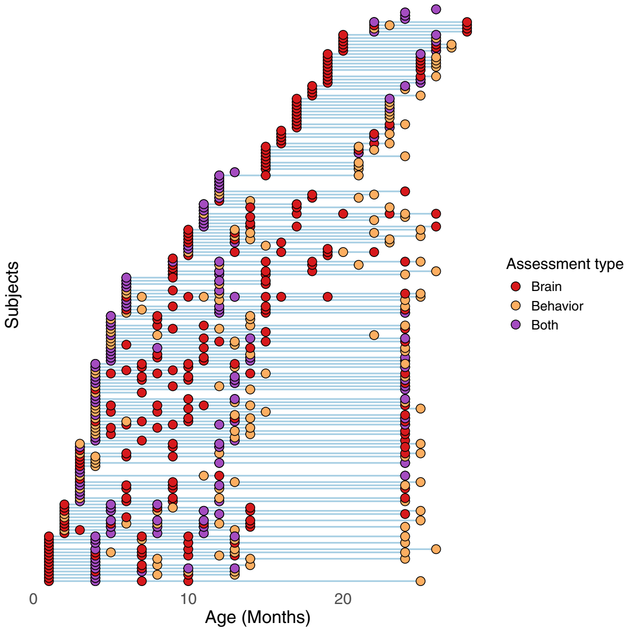

Figure 1. All data across all infants, ages, and assessment types. Red dots indicate a magnetic resonance imaging (MRI) assessment with high-quality data. Yellow dots indicate that behavioral data were available from either the Infant Behavior Questionnaire-Revised or Early Childhood Behavior Questionnaire. Purple dots indicate instances when at a single time point, an infant had both MRI and behavioral data available.

and coregistration to a T1- and T2-weighted reference using boundary-based registration.

Confounds in the preprocessed blood oxygen level–dependent (BOLD) time series were identified and utilized for denoising. These confounds included head-motion estimates and framewise displacement (FD) [computed using absolute sum of relative motions (53)], as well as whole-brain global signal. Frames that exceeded a threshold of 0.25 mm FD or 1.5 standardized root mean square of temporal fMRI signal change at each time point (DVARS) were annotated as motion outliers. The BOLD time series was then resampled into standard space, which produced a preprocessed BOLD time series in MNI infant space. Nongridded (surface) resamplings were performed using mri_vol2surf (infant FreeSurfer).

Denoising. Following visual inspection, custom python scripts denoised the data by scrubbing censored frames and regressing out the following nuisance variables: 24 head-motion parameters, motion outliers, CSF, WM, global signal, cosines, and pre–steady state outliers. This set of nuisance regressors has been shown to substantially attenuate artifacts in resting-state data (54). Low-frequency drifts were removed by the inclusion of cosines as nuisance regressors; this method is akin to bandpass filtering (55). Global signal regression was utilized in denoising because it has been shown to effectively remove respiration and motion artifacts (53,56).

Quality Control and Data Loss. To ensure that all processed data were high quality, quality assessment reports were visually inspected for all 518 MRI sessions. Following visual inspection, 77 MRI sessions (15%) were subsequently deemed to be poor quality. Twenty-seven sessions were outside the age range of 0 to 28 months for focal analyses and were thus removed. Of the remaining 414 sessions, 18 sessions had $<$250 frames of low-motion data. Thus, 396 MRI sessions were deemed to be high quality. These 396 MRI sessions came from 180 infants. Averaging across all participants and sessions, our high-quality MRI sample had approximately 11.57 minutes of data (mean = 867.67 retained frames, SD = 370.10 frames) (see the Supplement for distribution). There were no associations between the number of retained frames and age ($p > .565$).

To estimate the relative motion remaining in our high-quality sample, we computed the average FD in retained frames across all infants and across all ages ($\text{mean}_{\text{FD}} = 0.14$, $\text{SD}_{\text{FD}} = 0.017$) (see Figure S2 for average by age). While mean FD was low, there was a positive association between age and mean FD ($F_1 = 15.731$, $p < .001$) (see Figure S1). Thus, mean FD was controlled in our models.

Group Independent Component Analysis

To identify the brain networks of interest, we utilized MELODIC. MELODIC decomposed resting-state data into spatial and temporal components. Our dataset included different numbers of runs per participant and multiple imaging sessions; thus, to ensure that our group map was not biased toward individuals or time points with more available data we constrained the dataset used to generate the group maps. Specifically, every participant who contributed to the group map contributed 2 runs of resting-state data at 1 longitudinal time point, and each imaging assessment age was represented. Thus, all infants/time points contributed equally to the group network identification process. No significant age effects emerged for any group map (*p*s $>$.05), confirming that the correspondence with the within-network mask did not vary as a function of age. Thirty components were identified, and after visual inspection, 17 were classified as noise (due to inclusion of nonbrain tissue) and removed. We selected components that aligned most closely with the SN, FPN, DAN, and DMN by visual inspection (see the Supplement for details). Figure 2 illustrates spatial maps for the attention-related brain networks of interest. Notably, we found 2 networks that were largely anchored in the prefrontal cortex (PFC) and included some limited parietal regions; both have been labeled FPN (I and II, respectively). FPN II includes more lateral PFC than FPN I, while FPN I encompasses more anterior and medial portions of the PFC. Additionally, the infant DMN did not present with a frontal component, consistent with previous work (57). Additional details on the anatomical regions highlighted in the group maps are provided in the Supplement.

Following MELODIC, we conducted dual regression to extract participant-specific time series from the group map. Using the participant-specific time courses as input, we then conducted network modeling using FSLNets functions to compute Pearson correlations between all networks. Fisher's *r*-to-*z* transformation was applied. A group-level rsFC matrix with hierarchical clustering is presented in Figure 3. FSLNet's clustering algorithm detected 4 clusters. Cluster 1 comprises the 2 FPN components (independent component [IC] 3 and IC

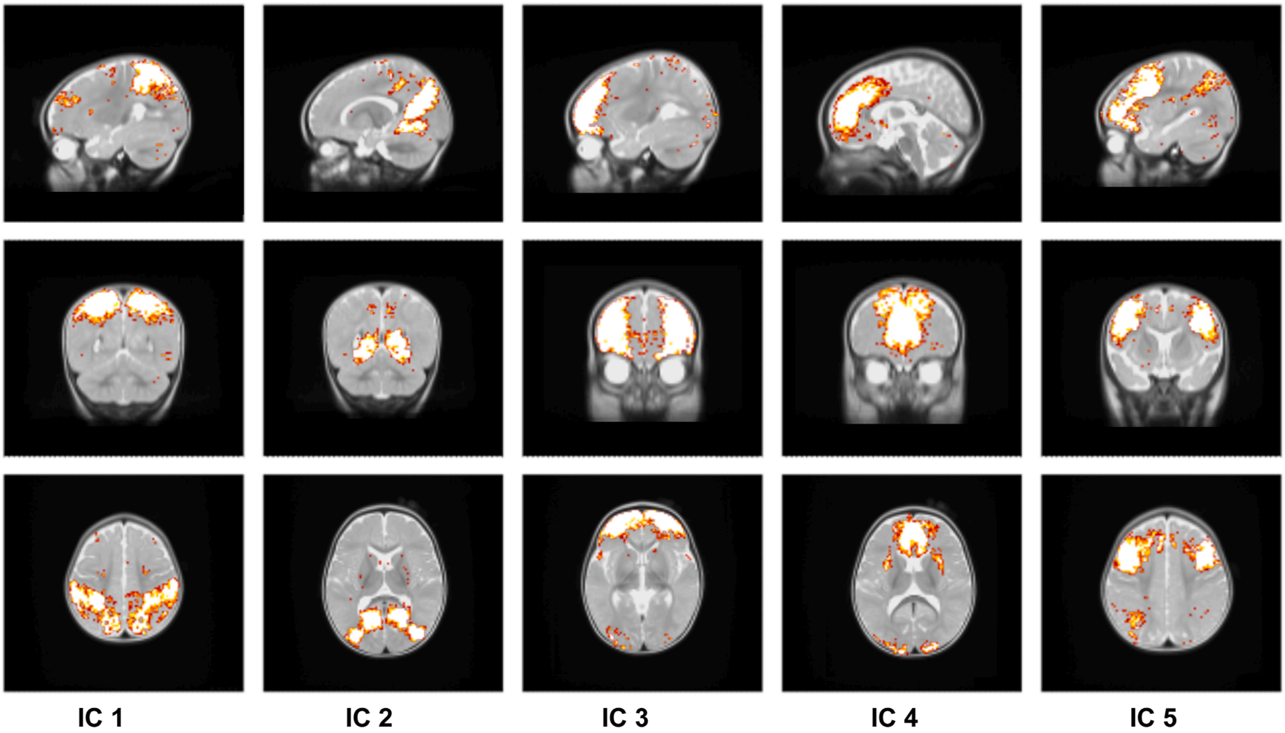

Figure 2. Spatial maps for the 5 independent components (ICs) selected for this analysis to represent dorsal attention network (IC 1), default mode network (IC 2), salience network (IC 4 [medial prefrontal cortex]), and frontoparietal network (FPN) (IC 3 [FPN I], IC 5 [FPN II]).

5). Cluster 2 comprises the DAN (IC 1). Cluster 3 comprises the SN (IC 4). Cluster 4 comprises the DMN (IC 2). Consistent with other work, we found that 1) the FPN is negatively associated with the DMN, 2) FPN II was negatively associated with SN/ventral attention network, and 3) the DAN, SN, and DMN were all negatively correlated with one another (57).

Parent Report of Infant Fearful Temperament

Parents reported on infant temperament using the Infant Behavior Questionnaire-Revised (IBQ-R) and the Early Childhood Behavior Questionnaire (ECBQ) (49). All analyses were conducted using the IBQ-R and ECBQ's fear subscales, which indicate the extent to which infants exhibit fear in the presence of novelty. The fear subscale of the ECBQ is considered equivalent to that of the IBQ, given the identical format and similar question structure, which facilitates a seamless age extension from the IBQ to the ECBQ (58,59). IBQ-R fear data were collected at 3 to 5 months (n = 68), 6 to 8 months (n = 32), 9 to 11 months (n = 20), and 12 to 15 months (n = 85). ECBQ fear data were collected at 20 to 27 months (n = 101). A total of 93 participants provided fearful temperament data at 2 or more time points, and 57 of them contributed data from at least 2 time points, including at least one after age 20 months. For the distribution of all available fear data, see the Supplement. ECBQ fear at 20 to 27 months (referred to throughout as age 2) was selected as the outcome for study aim 2 because this was the time point with the largest amount of parent-reported fear data. Study aim 3's analyses (examining co-trajectories of rsFC and fearful temperament) utilized all available IBQ and ECBQ data.

Analytic Approach

Aim 1 was to identify age-related changes in rsFCs between the SN, FPN (FPN I and FPN II), DAN, and DMN. Thus, we used the average spatial map from the second stage of dual regression to test for age effects on rsFC. All statistical analyses adjusted for mean FD and sex. Statistical significance was determined using Permutation Analysis of Linear Models (PALM) (60). PALM performs permutation-based inference, providing a robust method for statistical inference without relying on traditional parametric assumptions. All models were run with 500 permutations. The p values were computed after fitting a generalized Pareto distribution to the tail of the permutation distribution (61) to dispense with the need of performing a computationally prohibitively large number of permutations.

Aim 2 was to evaluate whether network changes related to age 2 fearfulness. Thus, for each attention network pair that showed a significant group-level age-related change (DAN-FPN II, DMN-SN), we first extracted participant-level rsFC intercept and slopes using linear mixed-effects models, implemented in R version 4.4.0 with the lme4 package (62).

Specifically, for each network pair, we estimated a linear mixed-effects model for the rsFC value, including participant-level random effects for both the intercept and the age term, and extracted the participant-level random intercepts and slopes for subsequent analysis. To model the age effect, we

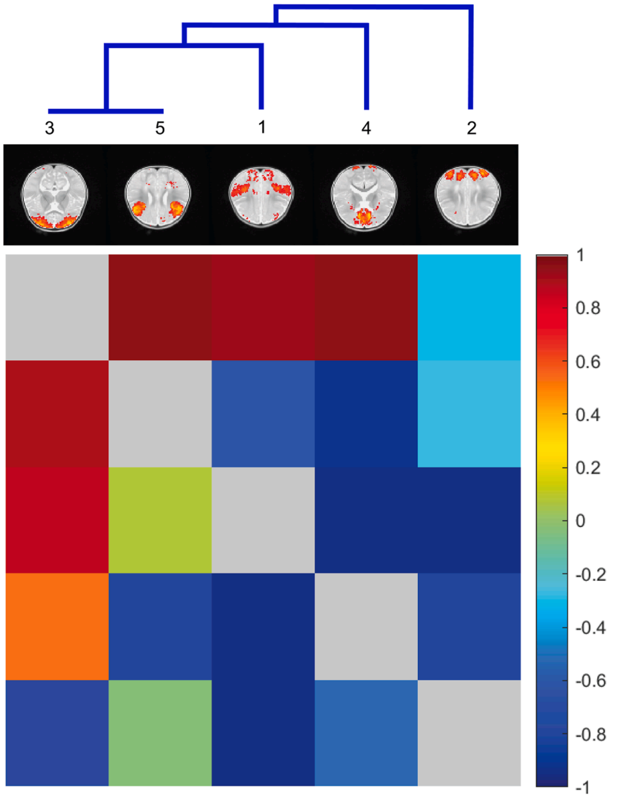

Figure 3. Group-level functional resting-state functional connectivity matrix of resting-state data. Full correlations are presented below the diagonal; partial correlations are presented above the diagonal. Four clusters emerged. Cluster components with more similar time courses are closer together.

considered both age and log(age) and selected the better representation based on the Akaike information criterion (AIC). The model with the lower AIC is reported below (see the Supplement for model fit comparison). The intercept and slope were then related to fear through linear regressions, with the participant-level intercept and slope included as a predictor in separate models for fear at age 2. *p* Values (threshold set at .05) for fixed effects were obtained using permutation tests with 10,000 permutations.

Aim 3 was to explore longitudinal co-trajectories of rsFC and fear across all network pairs and data collection time points, using longitudinal structural equation models (SEMs). Specifically, for each network pair, we tested the association between network rsFC and fearful temperament in terms of both their initial (intercept) and age-related changes (slope). Given each network pair, this approach jointly estimates the linear trajectory of the corresponding rsFC measures and that of fear, allowing for their longitudinal correlations through shared random effects (63,64). This longitudinal SEM with participant-level random intercepts and slopes is well suited to accommodating irregular time intervals, mismatch between FC and fear measurements, and handling missing data and allowed us to assess the association between changes in each rsFC measure and fear. Given the relatively small sample size for longitudinal assessments of both rsFC and fear, we estimated the models using a Bayesian paradigm for model stability (see the Supplement for additional details). This approach allowed us to include 167 participants with at least 1 nonmissing value for both FC and fear measures. To ensure model estimation stability, we utilized weakly informative prior, which shrink estimates toward the null (i.e., conservative), thereby avoiding overfitting of the longitudinal bivariate associations over time. The significance of FC-fear associations were assessed through the model parameters that captured the bivariate association (represented by the gamma parameters; see the Supplement for information) and their credible intervals.

RESULTS

Characterizing Attention-Related Network Change Over Time

On average, significant age-related rsFC decreases manifested in DAN-FPN II (η^2 = 0.13, familywise error rate–corrected p [p_{FWER}] $<$ .045) (Figure 4) and DMN-SN (η^2 = 0.10, $p_{\mathrm{FWER}} < .021$) (Figure 4)[a]. No other significant changes were observed.

rsFC Slopes Associated With 2-Year Fear

Next, we related both DAN-FPN II and DMN-SN rsFC age-related slopes to fear at age 2 years. The slope of DAN-FPN II rsFC significantly related to fear at age 2 (F_1 = 4.1993, β = 2.881, p = .043) (Figure 5), such that smaller decreases in DAN-FPN II rsFC over time were associated with greater fear at 2 years. No other significant associations emerged.

Longitudinal Modeling of the Co-Trajectories of rsFC and Fear Across Time

Next, we examined associations between rsFC trajectories and fear trajectories (i.e., slopes and intercepts). The rate of change in fear (slope) had moderate positive associations with 1) initial DAN-FPN II rsFC values (intercept), such that higher initial DAN-FPN II rsFC related to steeper increases in fear, with a posterior probability of the corresponding gamma parameter: $\Pr(\Gamma_{10} > 0) = 75\%$; and 2) the rate of change in DAN-FPN II rsFC value (slope), such that lower decreases in DAN-FPN II rsFC related to steeper increases in fear, with a posterior probability of the corresponding parameter: $\Pr(\Gamma_{11}) = 80\%$ (see Figure 6). Additionally, results demonstrated that the rate of change in fear (slope) had a moderate negative association with initial DAN-SN rsFC values (intercept), such that lower initial DAN-SN rsFC related to steeper increases in fear, with a posterior probability of the corresponding parameter: $\Pr(\Gamma_{10} < 0) = 80\%$. No other associations were observed.

DISCUSSION

This study characterized rsFC change over the first 2 years of life. Results showed age-related decreases in DMN-SN and DAN-FPN rsFC values. Smaller DAN-FPN declines related to greater fearful temperament at age 2. Longitudinal analyses

---

[a] η^2 represents the proportion of variance explained by age factor.

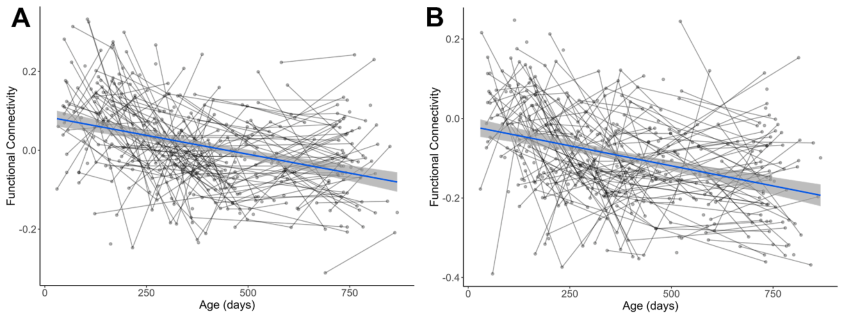

Figure 4. Postnatal age-related decreases were observed in dorsal attention network–frontal parietal network II **(A)** and default mode network–salience network **(B)** resting-state functional connectivities over the first 2 years of life.

leveraging all data replicated these focal findings within a Bayesian statistical framework; again, smaller reductions in DAN-FPN rsFC related to increases in fearfulness. Our longitudinal analyses also demonstrated that greater newborn DAN-FPN rsFC (i.e., intercept) was associated with increasing fearfulness. Furthermore, lower newborn DAN-SN rsFC was associated with increases in fearfulness. Together, this provides novel evidence that infant attention-related brain networks relate to the development of fearful temperament.

While previous work found decreasing DMN-SN and SN-FPN rsFC over the first years of life (6), our study is the first to show decreasing DAN-FPN rsFC. This provides additional evidence that attention-related brain networks specialize with development. During early infancy, high rsFC among networks suggests broadly coordinated brain activity (i.e., less network specialization), which decreases as each network becomes better defined (i.e., more specialized). Neural specialization could support attentional efficiency, consistent with research showing improved attention regulation across the first years of life (65,66). Age-related decreases in rsFC between the DMN and SN appeared robust to analytic methods. In adults, the SN modulates the balance between the DMN and FPN to detect external stimuli and evaluate it based on internal processes (34,67). If the DMN functions similarly in infants and adults, such rsFC changes between the DMN and SN could relate to infants' increases in regulatory capacity with maturation in attentional control (6,68).

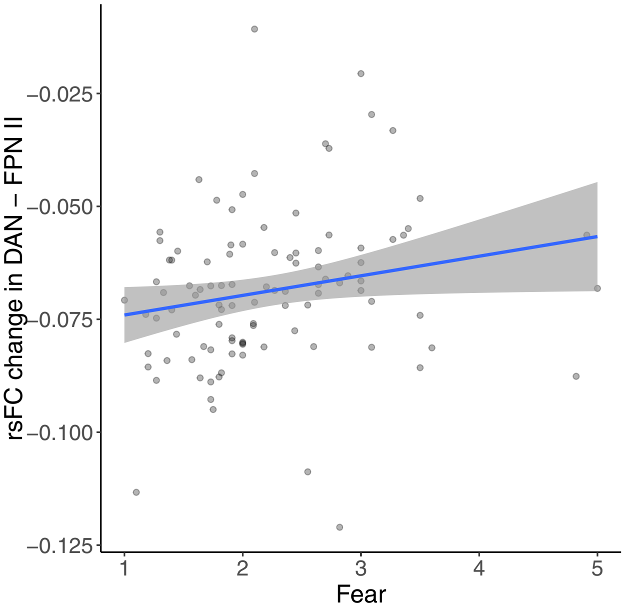

Figure 5. Positive association between resting-state functional connectivity (rsFC) rate of change in dorsal attention network (DAN)–frontal parietal network (FPN) II and fear at 2 years.

By using a novel Bayesian analytic method, we were able to explore how rsFC trajectories relate to the maintenance of fearful temperament over the first 2 years of life. Our results implicated greater initial DAN-FPN rsFC and lower initial DAN-SN rsFC in increasing fearfulness, resembling previous findings with newborns (9,12) and 4-month-old infants (8), as well as previous data on the neural correlates of anxiety symptoms in older individuals (3,68,69). While previous work has linked the SN and FPN to anxiety and its early-life risk factors (3,70,71), few studies have implicated the DAN. The DAN supports selective attention (72,73), and altered DAN rsFC has recently been linked to social anxiety disorders (74). The link between neonatal DAN-FPN rsFC and the maintenance of a fearful phenotype may suggest that attentional control is a core feature of early-life risk. These data are also consistent with theoretical models that emphasize the significance of time-limited experiences in infancy for developmental pathways to psychopathology (75).

In addition to newborn rsFC, we also found that smaller decreases in DAN-FPN rsFC were associated with greater fear. We showed this both by relating the rsFC slope for the DAN-FPN to fear at age 2 and by evaluating fearfulness trajectories. The convergence across these two analytic approaches is promising and suggests developmental stability in brain network alterations that may underlie anxiety-related behaviors (e.g., challenges with attentional control). By evaluating fearful temperament trajectories in relation to rsFC trajectories, these data are the first to demonstrate that changes in attention-related brain networks during infancy (particularly in networks that dynamically control attention and support top-down regulation) may underlie the maintenance of fear over time.

Taken together, our findings may suggest that infants who exhibit a more tightly coupled DAN-FPN system—and who show less change—may remain stuck in a vigilance-biased state, leaving fewer neural resources for salience-driven

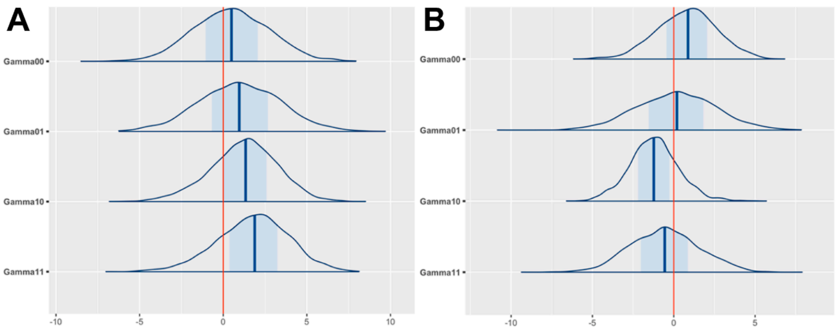

Figure 6. **(A)** Posterior distributions of gamma parameters for the association between fear and dorsal attention network (DAN)–frontoparietal network (FPN) II resting-state functional connectivity (rsFC); **(B)** posterior distributions of gamma parameters for the association between fear and DAN–salience network (SN) rsFC. Each panel represents bivariate longitudinal association parameter estimates from the longitudinal structural equation models for each network pair (DAN-FPN II and DAN-SN): 1) gamma$_{00}$ (intercept-intercept) captures the relationship between the fear intercept (initial value) and the FC intercept (initial value); 2) gamma$_{01}$ (intercept-slope) captures the relationship between the fear intercept and the FC time slope; 3) gamma$_{10}$ (slope-intercept) captures the relationship between the fear time slope and the FC intercept; and 4) gamma$_{11}$ (slope-slope) captures the relationship between the fear time slope and the FC time slope. The blue shaded regions represent 50% posterior credible intervals.

switching (SN) and introspective appraisal (DMN) that typically downregulate threat signals (76). If this is followed by a delay in developmental rebalancing among the DAN, FPN, SN, and DMN, fearfulness may increase and stabilize: Persistent DAN-FPN synchrony sustains hyperorienting to potential danger, while smaller DMN-SN decoupling limits the infant's capacity to flexibly disengage attention from aversive arousal and re-engage with positive social stimuli (77). This evidence is also consistent with several core neurodevelopmental theories of anxiety (15,17). However, additional work is needed to understand the extent to which these changes underlie the later development of anxiety symptomatology and to isolate environmental factors that could alter these trajectories.

The current study has several notable strengths. First, we utilized a publicly available dataset (BCP) that utilized a cohort-sequential design and provided high-quality rsFC data from 180 infants across 396 sessions. Previous studies estimated change by leveraging a few developmental anchor points (e.g., 0–3 months, 1 year, 2 years) (6,11). However, the BCP captured variability across the period from 0 to 2 years with nearly all months included. Second, our data-driven approach to network identification avoided assuming an adult-like organization for the infant brain, thereby generating an unbiased group map. Third, this article includes traditional regression analyses using behavioral data at age 2 (i.e., the time point when most participants had fearful temperament data). However, we supplemented these analyses using an advanced Bayesian approach, and the consistency of our findings from these supplemental analyses illustrate that our results are robust.

These strengths should be considered together with the study's limitations. First, the correlational nature of the analysis limits interpretations related to the causality or directionality of the associations between rsFC changes and fearful temperament. Future longitudinal studies are needed to advance understanding of how developmental changes in attention networks relate to anxiety outcomes. Second, we focused on 4 key attention-related networks. Thus, it is possible that rsFC among other brain networks (e.g., visual, sensorimotor, auditory) (3,74) may also play a role in the development of fearfulness. It is also possible that if we had focused on amygdala rsFC, as has been reported previously (11), our conclusions might be different. Future research is needed to evaluate this possibility. Third, we utilized parent-report measures of fearfulness. While these questionnaires provided an efficient assessment of early temperament development for the collection of longitudinal data, we know that parent report and observed behavior are only modestly correlated (78,79). Thus, extensions using observational methods should be conducted to better understand the generalizability of these results. Fourth, although independent component analysis (ICA) avoids assumptions of adult brain functional organization, our results are highly dependent on our network identification process. We provide considerable evidence of the regions that make up each network both in the main text and the Supplement. We caution that our results should be considered in relation to the precise regions captured by our ICA group maps. However, the consistency between our findings and published work that used atlas-based approaches may minimize this concern. Additional large-scale longitudinal MRI studies could help determine the reproducibility of these data-driven networks. Finally, the sample reported on here is largely non-Hispanic White, highly educated, and of high socioeconomic status. Replicating these findings in more diverse samples is critical.

Conclusions

This study provides novel insights into the development of attention-related brain networks during infancy and how brain change relates to fear during the first years of life. This work is both consistent with neurodevelopmental theories and provides a more nuanced understanding of rsFC changes that may relate to fear. By advancing our understanding of the neural origins of fear, a potent risk marker for developing anxiety, this work has the potential to inform early identification efforts and shape future work on the mechanisms that underlie effective early intervention.

ACKNOWLEDGMENTS AND DISCLOSURES

This work was supported by the National Institute of Mental Health (Grant Nos. R00MH125878 [to principal investigator (PI), CAF], R21MH122976 [to PI, NAF], R01MH104324 [to PI, JTE], U01MH110274 [to co-PI, JTE], K23MH130751 [to PI, EV]) and the Intramural NIMH Grant (Grant No. ZIA-MH002782 [to PI, DSP]).

We would like to acknowledge the families that made this research possible, and Isabella Schneider and Hannah Hardiman for their contributions to data cleaning.

A previous version of this article was published as a preprint on medRxiv: https://doi.org/10.1101/2025.01.24.25321085.

The authors report no biomedical financial interests or potential conflicts of interest.

ARTICLE INFORMATION

From the Department of Child and Adolescent Psychiatry, New York University Grossman School of Medicine, New York, New York (CAF, AM, JX); Department of Population Health, New York University Grossman School of Medicine, New York, New York (HGP); Department of Psychology, University of Southern California, Los Angeles, California (EV); Institute of Child Development, Department of Pediatrics, Masonic Institute for the Developing Brain, University of Minnesota, Minneapolis, Minnesota (JTE); Department of Human Development and Quantitative Methodology, University of Maryland, College Park, Maryland (DK, NAF); Emotion and Development Branch, National Institute of Mental Health, Bethesda, Maryland (DSP); and Division of Human Genetics, School of Medicine, University of Texas Rio Grande Valley, Brownsville, Texas (AW).

CAF and AM are joint first authors.

Address correspondence to Courtney A. Filippi, Ph.D., at courtney.filippi@nyulangone.org.

Received Mar 6, 2025; revised Jul 1, 2025; accepted Jul 11, 2025.

Supplementary material cited in this article is available online at https://doi.org/10.1016/j.bpsc.2025.07.003.

REFERENCES

1. Beesdo K, Knappe S, Pine DS (2009): Anxiety and anxiety disorders in children and adolescents: Developmental issues and implications for DSM-V. Psychiatr Clin North Am 32:483–524.
2. Strawn JR, Lu L, Peris TS, Levine A, Walkup JT (2021): Research Review: Pediatric anxiety disorders—What have we learnt in the last 10 years? J Child Psychol Psychiatry 62:114–139.
3. Perino MT, Yu Q, Myers MJ, Harper JC, Baumel WT, Petersen SE, *et al.* (2021): Attention alterations in pediatric anxiety: Evidence from behavior and neuroimaging. Biol Psychiatry 89:726–734.
4. Pine DS (2007): Research Review: A neuroscience framework for pediatric anxiety disorders. J Child Psychol Psychiatry 48:631–648.
5. Bar-Haim Y, Lamy D, Pergamin L, Van Bakermans-Kranenburg MJ, Van IJzendoorn MH (2007): Threat-related attentional bias in anxious and nonanxious individuals: A meta-analytic study. Psychol Bull 133:1–24.
6. Gao W, Alcauter S, Smith JK, Gilmore JH, Lin W (2015): Development of human brain cortical network architecture during infancy. Brain Struct Funct 220:1173–1186.
7. Filippi CA, Ravi S, Bracy M, Winkler A, Sylvester CM, Pine DS, Fox NA (2021): Amygdala functional connectivity and negative reactive temperament at Age 4 months. J Am Acad Child Adolesc Psychiatry 60:1137–1146.
8. Filippi CA, Winkler AM, Kanel D, Elison JT, Hardiman H, Sylvester C, *et al.* (2024): Neural correlates of novelty-evoked distress in 4-month-old infants: A synthetic cohort study. Biol Psychiatry Cogn Neurosci Neuroimaging 9:905–914.
9. Graham AM, Pfeifer JH, Fisher PA, Lin W, Gao W, Fair DA (2015): The potential of infant fMRI research and the study of early life stress as a promising exemplar. Dev Cogn Neurosci 12:12–39.
10. Ravi S, Catalina Camacho M, Fleming B, Scudder MR, Humphreys KL (2023): Concurrent and prospective associations between infant frontoparietal and default mode network connectivity and negative affectivity. Biol Psychol 184:108717.
11. Salzwedel AP, Stephens RL, Goldman BD, Lin W, Gilmore JH, Gao W (2019): Development of amygdala functional connectivity during infancy and its relationship with 4-year behavioral outcomes. Biol Psychiatry Cogn Neurosci Neuroimaging 4:62–71.
12. Sylvester CM, Smyser CD, Smyser T, Kenley J, Ackerman JJ, Shimony JS, *et al.* (2018): Cortical functional connectivity evident after birth and behavioral inhibition at Age 2. Am J Psychiatry 175:180–187.
13. Sylvester CM, Pine DS (2021): Pediatric anxiety disorders: Insights from basic neuroscience, development, and clinical research. Biol Psychiatry 89:638–640.
14. Filippi CA, Valadez EA, Fox NA, Pine DS (2022): Temperamental risk for anxiety: Emerging work on the infant brain and later neurocognitive development. Curr Opin Behav Sci 44:101105.
15. Bierstedt L, Reider LB, Burris JL, Vallorani A, Gunther KE, Buss KA, *et al.* (2022): Bi-directional relations between attention and social fear across the first two years of life. Infant Behav Dev 69:101750.
16. Morales S, Pérez-Edgar KE, Buss KA (2015): Attention biases towards and away from threat mark the relation between early dysregulated fear and the later emergence of social withdrawal. J Abnorm Child Psychol 43:1067–1078.
17. Pérez-Edgar K, Reeb-Sutherland BC, McDermott JM, White LK, Henderson HA, Degnan KA, *et al.* (2011): Attention biases to threat link behavioral inhibition to social withdrawal over time in very young children. J Abnorm Child Psychol 39:885–895.
18. Swales DA, Markant J, Hennessey EP, Glueck DH, Hankin BL, Davis EP (2023): Infant negative affectivity and patterns of affect-biased attention. Dev Psychobiol 65:e22380.
19. Clauss JA, Blackford JU (2012): Behavioral inhibition and risk for developing social anxiety disorder: A meta-analytic study. J Am Acad Child Adolesc Psychiatry 51:1066–1075.e1.
20. Gartstein MA, Bridgett DJ, Rothbart MK, Robertson C, Iddins E, Ramsay K, Schlect S (2010): A latent growth examination of fear development in infancy: Contributions of maternal depression and the risk for toddler anxiety. Dev Psychol 46:651–668.
21. Hirshfeld-Becker DR, Biederman J, Henin A, Faraone SV, Davis S, Harrington K, Rosenbaum JF (2007): Behavioral inhibition in preschool Children At Risk is a specific predictor of middle childhood social anxiety: A five-year follow-up. J Dev Behav Pediatr 28:225–233.
22. Hudson JL, Dodd HF, Bovopoulos N (2011): Temperament, family environment and anxiety in preschool children. J Abnorm Child Psychol 39:939–951.
23. Sandstrom A, Uher R, Pavlova B (2020): Prospective association between childhood behavioral inhibition and anxiety: A meta-analysis. J Abnorm Child Psychol 48:57–66.
24. Ver Pault M, Dai YG, Abel MR, Carter AS, Henin A, Kagan E, *et al.* (2024): Screening for fearful and shy temperament in toddlers predicts elevated anxiety symptoms: A prospective study. J Child Fam Stud 33:2110–2120.
25. Buss KA (2011): Which fearful toddlers should we worry about? Context, fear regulation, and anxiety risk. Dev Psychol 47:804–819.
26. Chronis-Tuscano A, Degnan KA, Pine DS, Perez-Edgar K, Henderson HA, Diaz Y, *et al.* (2009): Stable early maternal report of behavioral inhibition predicts lifetime social anxiety disorder in adolescence. J Am Acad Child Adolesc Psychiatry 48:928–935.
27. Braungart-Rieker JM, Hill-Soderlund AL, Karrass J (2010): Fear and anger reactivity trajectories from 4 to 16 months: The roles of temperament, regulation, and maternal sensitivity. Dev Psychol 46:791–804.
28. Carranza JA, González-Salinas C, Ato E (2013): A longitudinal study of temperament continuity through IBQ, TBAQ and CBQ. Infant Behav Dev 36:749–761.
29. Gartstein MA, Hancock GR, Iverson SL (2018): Positive affectivity and fear trajectories in infancy: Contributions of mother–child interaction factors. Child Dev 89:1519–1534.
30. Auday ES, Taber-Thomas BC, Pérez-Edgar KE (2018): Neural correlates of attention bias to masked facial threat cues: Examining children at-risk for social anxiety disorder. Neuroimage Clin 19:202–212.
31. Fu X, Taber-Thomas BC, Pérez-Edgar K (2017): Frontolimbic functioning during threat-related attention: Relations to early behavioral inhibition and anxiety in children. Biol Psychol 122:98–109.
32. Harrewijn A, Cardinale EM, Groenewold NA, Bas-Hoogendam JM, Aghajani M, Hilbert K, *et al.* (2021): Cortical and subcortical brain structure in generalized anxiety disorder: Findings from 28 research sites in the ENIGMA-Anxiety Working Group. Transl Psychiatry 11:502.
33. Menon B (2019): Towards a new model of understanding—The triple network, psychopathology and the structure of the mind. Med Hypotheses 133:109385.
34. Menon V (2011): Large-scale brain networks and psychopathology: A unifying triple network model. Trends Cogn Sci 15:483–506.

35. White LK, Britton JC, Sequeira S, Ronkin EG, Chen G, Bar-Haim Y, *et al.* (2016): Behavioral and neural stability of attention bias to threat in healthy adolescents. Neuroimage 136:84–93.
36. Schimmelpfennig J, Topczewski J, Zajkowski W, Jankowiak-Siuda K (2023): [cited Nov 5 2024]. The role of the salience network in cognitive and affective deficits. Front Hum Neurosci, Internet 17:1133367.
37. Corbetta M, Patel G, Shulman GL (2008): The reorienting system of the human brain: From environment to theory of mind. Neuron 58:306–324.
38. Scolari M, Seidl-Rathkopf KN, Kastner S (2015): Functions of the human frontoparietal attention network: Evidence from neuroimaging. Curr Opin Behav Sci 1:32–39.
39. Menon V (2013): Developmental pathways to functional brain networks: Emerging principles. Trends Cogn Sci 17:627–640.
40. Smith SM, Fox PT, Miller KL, Glahn DC, Fox PM, Mackay CE, *et al.* (2009): Correspondence of the brain's functional architecture during activation and rest. Proc Natl Acad Sci U S A 106:13040–13045.
41. Raichle ME (2015): The brain's default mode network. Annu Rev Neurosci 38:433–447.
42. Menon V (2023): 20 years of the default mode network: A review and synthesis. Neuron 111:2469–2487.
43. Lucherini Angeletti L, Scalabrini A, Ricca V, Northoff G (2023): Topography of the anxious self: Abnormal rest-task modulation in social anxiety disorder. Neuroscientist 29:221–244.
44. Nielsen AN, Graham AM, Sylvester CM (2023): Baby brains at work: How task-based functional magnetic resonance imaging can illuminate the early emergence of psychiatric risk. Biol Psychiatry 93:880–892.
45. Sylvester CM, Myers MJ, Perino MT, Kaplan S, Kenley JK, Smyser TA, *et al.* (2021): Neonatal brain response to deviant auditory stimuli and relation to maternal trait anxiety. Am J Psychiatry 178:771–778.
46. Schwarzlose RF, Filippi CA, Myers MJ, Harper J, Camacho MC, Smyser TA, *et al.* (2024): Neonatal neural responses to novelty related to behavioral inhibition at 1 year. Dev Psychol 60:2062–2070.
47. Thomas E, Buss C, Rasmussen JM, Entringer S, Ramirez JSB, Marr M, *et al.* (2019): Newborn amygdala connectivity and early emerging fear. Dev Cogn Neurosci 37:100604.
48. Alcauter S, Lin W, Keith Smith J, Gilmore JH, Gao W (2015): Consistent anterior–posterior segregation of the insula during the first 2 years of life. Cereb Cortex 25:1176–1187.
49. Howell BR, Styner MA, Gao W, Yap PT, Wang L, Baluyot K, *et al.* (2019): The UNC/UMN Baby Connectome Project (BCP): An overview of the study design and protocol development. Neuroimage 185:891–905.
50. Pruett JR, Kandala S, Hoertel S, Snyder AZ, Elison JT, Nishino T, *et al.* (2015): Accurate age classification of 6 and 12 month-old infants based on resting-state functional connectivity magnetic resonance imaging data. Dev Cogn Neurosci 12:123–133.
51. Fonov V, Evans AC, Botteron K, Almli CR, McKinstry RC, Collins DL, Brain Development Cooperative Group (2011): Unbiased average age-appropriate atlases for pediatric studies. Neuroimage 54:313–327.
52. Sanchez CE, Richards JE, Almli CR (2012): Age-specific MRI templates for pediatric neuroimaging. Dev Neuropsychol 37:379–399.
53. Power JD, Mitra A, Laumann TO, Snyder AZ, Schlaggar BL, Petersen SE (2014): Methods to detect, characterize, and remove motion artifact in resting state fMRI. Neuroimage 84:320–341.
54. Satterthwaite TD, Elliott MA, Gerraty RT, Ruparel K, Loughead J, Calkins ME, *et al.* (2013): An improved framework for confound regression and filtering for control of motion artifact in the preprocessing of resting-state functional connectivity data. Neuroimage 64:240–256.
55. Hallquist MN, Hwang K, Luna B (2013): The nuisance of nuisance regression: Spectral misspecification in a common approach to resting-state fMRI preprocessing reintroduces noise and obscures functional connectivity. Neuroimage 82:208–225.
56. Li J, Kong R, Liégeois R, Orban C, Tan Y, Sun N, *et al.* (2019): Global signal regression strengthens association between resting-state functional connectivity and behavior. Neuroimage 196:126–141.
57. Gao W, Gilmore JH, Shen D, Smith JK, Zhu H, Lin W (2013): The synchronization within and interaction between the default and dorsal attention networks in early infancy. Cereb Cortex 23:594–603.
58. Gartstein MA, Rothbart MK (2003): Studying infant temperament via the Revised Infant Behavior Questionnaire. Infant Behav Dev 26:64–86.
59. Putnam SP, Helbig AL, Gartstein MA, Rothbart MK, Leerkes E (2014): Development and assessment of short and very short forms of the Infant Behavior Questionnaire–Revised. J Pers Assess 96:445–458.
60. Winkler AM, Ridgway GR, Webster MA, Smith SM, Nichols TE (2014): Permutation inference for the general linear model. Neuroimage 92:381–397.
61. Winkler AM, Ridgway GR, Douaud G, Nichols TE, Smith SM (2016): Faster permutation inference in brain imaging. Neuroimage 141:502–516.
62. Bates D, Mächler M, Bolker B, Walker S (2015): Fitting linear mixed-effects models using lme4. J Stat Soft 67:1–48.
63. Felt JM, Depaoli S, Tiemensma J (2017): Latent growth curve models for biomarkers of the stress response. Front Neurosci 11:315.
64. Muniz-Terrera G, Robitaille A, Kelly A, Johansson B, Hofer S, Piccinin A (2017): Latent growth models matched to research questions to answer questions about dynamics of change in multiple processes. J Clin Epidemiol 82:158–166.
65. Forest TA, Amso D (2023): Neurodevelopment of attention, learning, and memory systems in infancy. Annu Rev Dev Psychol 5:45–65.
66. Hendry A, Johnson MH, Holmboe K (2019): Early development of visual attention: Change, stability, and longitudinal associations. Annu Rev Dev Psychol 1:251–275.
67. Brown CA, Schmitt FA, Smith CD, Gold BT (2019): Distinct patterns of default mode and executive control network circuitry contribute to present and future executive function in older adults. Neuroimage 195:320–332.
68. Zhang H, Shen D, Lin W (2019): Resting-state functional MRI studies on infant brains: A decade of gap-filling efforts. Neuroimage 185:664–684.
69. Liu X, Zheng G, Wang X, Li Y, Ji S, Zhang Y, *et al.* (2022): The brain activation of anxiety disorders with emotional stimuli-An fMRI ALE meta-analysis. Neurocase 28:448–457.
70. Hilbert K, Adolph D, Arolt V, Bischoff S, Böhnlein J, *et al.* (2025): Resting-state functional connectivity in anxiety disorders: A multicenter fMRI study. Mol Psychiatry 30:1548–1557.
71. Zugman A, Jett L, Antonacci C, Winkler AM, Pine DS (2023): A systematic review and meta-analysis of resting-state fMRI in anxiety disorders: Need for data sharing to move the field forward. J Anxiety Disord 99:102773.
72. Rajan A, Meyyappan S, Liu Y, Samuel IBH, Nandi B, Mangun GR, Ding M (2021): The microstructure of attentional control in the dorsal attention network. J Cogn Neurosci 33:965–983.
73. Spreng RN, Sepulcre J, Turner GR, Stevens WD, Schacter DL (2013): Intrinsic architecture underlying the relations among the default, dorsal attention, and frontoparietal control networks of the human brain. J Cogn Neurosci 25:74–86.
74. Zhang X, Yang X, Wu B, Pan N, He M, Wang S, *et al.* (2023): Large-scale brain functional network abnormalities in social anxiety disorder. Psychol Med 53:6194–6204.
75. Ostlund B, Pérez-Edgar K (2023): Two-hit model of behavioral inhibition and anxiety. Annu Rev Dev Psychol 5:239–261.
76. Li X, Chen H, Hu Y, Larsen RJ, Sutton BP, McElwain NL, Gao W (2023): Functional neural network connectivity at 3 months predicts infant-mother dyadic flexibility during play at 6 months. Cereb Cortex 33:8321–8332.
77. Hu Y, Chen H, Li X, Larsen RJ, Sutton BP, Gao W, McElwain NL (2024): Associations between infant amygdala functional connectivity and social engagement following a stressor: A preliminary investigation. Dev Sci 27:e13418.
78. Freund JD (2019): Early temperament in parental report and scientific observation. Early Child Dev Care 189:2318–2333.
79. Faísca L, Ferreira LI, Fernandes CC, Gagne JR, Martins AT (2021): Behavioral inhibition in childhood: European Portuguese adaptation of an observational measure (lab-TAB). Children (Basel) 8:162.